Proteomics Study on the Cerebrospinal Fluid of Patients with Encephalitis

Liu-Lin Xiong,[⊥] Lu-Lu Xue,[⊥] Yan-Jun Chen, Ruo-Lan Du, Qian Wang, Song Wen, Lin Zhou, Tao Liu, Ting-Hua Wang,* and Chang-Yin Yu*

Read Online

ACCESS | Metrics & More | Article Recommendations

ABSTRACT: Objective: Label-free quantitative proteomics was applied to analyze differentially expressed proteins (DEPs) in the cerebrospinal fluid (CSF) of patients with encephalitis. The database was used to screen for possible biomarkers in encephalitis, followed by validation and preliminary investigation of the role of some DEPs in the pathogenesis of encephalitis using enzyme-linked immunosorbent assay (ELISA). Methods: We performed label-free quantitative proteomics on 16 cerebrospinal fluid samples (EM group, encephalitis with mental and behavioral disorders patients, n = 5; NED group, encephalitis without mental and behavioral disorders patients, n = 6; N group, healthy individuals, n = 5). The extracted CSF proteins were examined by mass spectrometry and enzymatic digestion and detected using protein profiling and data analysis. Interproscan was used to perform Gene Ontology (GO) and Kyoto Encyclopedia of Genes and Genomes (KEGG) pathway enrichment analysis of the DEPs. ELISA was used to verify the changes in the levels of some DEPs in the CSF. Results: A total of 941 proteins were found to be significantly differentially expressed, including 250 upregulated DEPs and 691 downregulated DEPs. GO analysis suggested that there were six enriched functions that intersect among the EM, NED, and N groups, including synapse organization, membrane, integral component of membrane, membrane part, G-protein-coupled receptor signaling pathway, and transmembrane signaling receptor activity. KEGG analysis revealed that there were three signaling pathways that intersect among the EM, NED, and N groups, including fructose and mannose metabolism, inositol phosphate metabolism, and Jak-STAT signaling pathway. Furthermore, four downregulated encephalitis-related neurological synapse proteins were identified after screening for differentially expressed proteins, including NRXN3, NFASC, LRRC4B, and NLGN2. The result of ELISA further verified that the expression of NLGN2 and LRRC4B was obviously higher in the NED group than in the N group. Conclusions: These findings demonstrated that NLGN2 and LRRC4B proteins were upregulated in the NED group and could be potential biomarkers for the diagnosis of encephalitis, but still needs a lot of multiomics studies to be used in clinical.
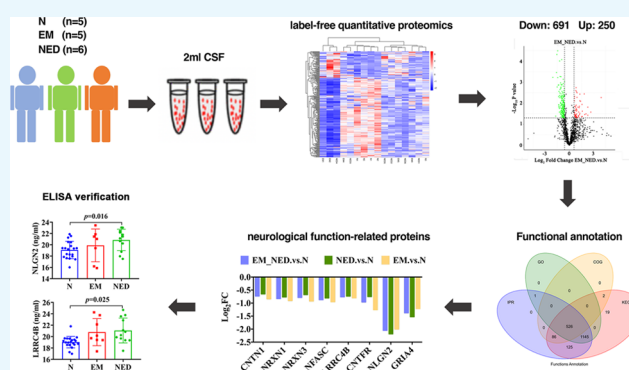
INTRODUCTION

Encephalitis is an inflammatory lesion of the brain parenchyma caused by the invasion of pathogens, which caused synaptic damage to neurons in the brain. It is characterized clinically by systemic toxemia and neurological symptoms, such as high fever, headache, vomiting, disturbance of consciousness, meningeal irritation signs, etc.[1−3] Cerebrospinal fluid (CSF) is a clear, colorless fluid that fills the ventricles, subarachnoid space, and central canal of the spinal cord, circulating on the surface of the brain and spinal cord.[4] In addition, CSF contains proteins, enzymes, and a number of other physiologically important substances whose changes can reflect pathological processes in central nervous system diseases.[5,6] Therefore, the study of CSF differential expressed proteins is significant for the discovery of brain disease biomarkers.[7−9]

Moreover, proteomic analysis is an advanced method to detect proteins in various biological materials, such as serum, urine, saliva, seminal plasma, tears, CSF, bronchoalveolar lavage fluid, or tissue. Using two-dimensional electrophoresis, mass spectrometry, bioinformatics, and databases, proteomic analysis provides the tools to systematically and comprehensively study the changes in CSF protein levels due to disease.[10−12] Consequently, in this study, our team will perform a proteomic study of CSF on encephalitis with mental

and behavioral disorders patients, encephalitis without mental and behavioral disorders patients, and healthy individuals. The aim of this study was to compare the differentially expressed proteins of CSF samples among the three groups mentioned above and sought to investigate the proteomic differences between encephalitis patients and normal subjects.

■ METHODS

Patient Samples. The CSF samples were obtained from the Affiliated Hospital of Zunyi Medical University following approval by the Ethics Committee of the Affiliated Hospital of Zunyi Medical University. The study was conducted in accordance with the principles of the Declaration of Helsinki. Five of healthy individuals (N group), five of encephalitis with mental and behavioral disorders patients (EM group), and six of encephalitis without mental and behavioral disorders patients (NED group) were recruited in the study. Their CSF samples were used for label-free quantitative proteomics. In addition, a total of 40 people were recruited for further enzyme-linked immunosorbent assay (ELISA) validation, including 20 healthy individuals, 8 EM patients, and 12 NED patients.

The patient was placed in the left lateral position, and the lumbar 3 and 4 (L3−L4) intervertebral space was taken as the puncture site. After routine disinfection, local infiltration anesthesia was applied to the L3−L4 positions. The puncture needle was inserted vertically from the puncture point, and after the obvious feeling of falling, the needle core was withdrawn, and the five-colored clear CSF was seen to flow out slowly. CSF (2 mL) was retained and centrifuged at 4 °C for 10 min at 2000g and then stored in a −80 °C refrigerator.

CSF Protein Extraction and Quantification. After thawing, 2 mL of CSF was placed in a test tube, mixed upside down with trichloroacetic acid (TCA)/ice acetone solution, and left overnight at −20 °C. The next day, it was taken out and centrifuged at 12 000 rpm and 4 °C for 30 min, the supernatant was discarded, and the precipitate was controlled and dried. The precipitate was washed three times with 90% acetone, centrifuged, the supernatant was discarded, and the precipitate was dried for 5 min. The protein was then lysed by adding lysis solution (6 mol/L urea, 100 mM triethylammonium bicarbonate (TEAB), pH = 8.5) to the precipitate and centrifuged for 10 min at 12 000 rpm, 4 °C, and the supernatant was taken as the sample to be measured.

After protein lysis and proteolysis, the protein concentration of the sample was determined by Bradford Protein Quantification Kit, and the bovine serum albumin (BSA) standard protein solution was prepared according to the instruction, and the concentration gradient was 0−0.5 μg/μL. The BSA standard protein solution and the sample solution to be tested at different dilutions were added into the 96-well plate in different concentration gradients to make up the volume to 20 μL, and each gradient was repeated three times. Then, 180 μL of G250 staining solution was added rapidly, left at room temperature for 5 min, and the absorbance at 595 nm was measured. The absorbance of the standard protein solution was used to plot the standard curve and calculate the protein concentration of the sample to be measured. Then, 20 μg of each sample was subjected to 12% sodium dodecyl sulfate-polyacrylamide gel electrophoresis (SDS-PAGE) at 80 V for 20 min for the concentrated gel and 120 V for 90 min for the separated gel. After the electrophoresis, the samples were

stained with Kemas Brilliant Blue R-250 and decolorized until the bands were clear.

CSF Protein Digestion. The protein samples were digested by adding 1.5 μg of trypsin and 500 μL of 100 mM TEAB buffer at 37 °C for 4 h. Then, 1.5 ug of trypsin and CaCl$_2$ were added overnight. Formic acid was added to adjust the pH to less than 3. The sample was mixed and centrifuged at 12 000g for 5 min at room temperature, and the supernatant was slowly passed through the C18 desalting column, followed by washing solution (0.1% formic acid, 3% acetonitrile) three times, then adding an appropriate amount of eluent (0.1% formic acid, 70% acetonitrile), collecting the filtrate, and lyophilizing.

Protein Profiling. The mobile phases A (100% water, 0.1% formic acid) and B (80% acetonitrile, 0.1% formic acid) were prepared. The lyophilized powder was dissolved in 10 μL of liquid A, centrifuged at 14 000g for 20 min at 4 °C, and 1 μg of supernatant was injected into the sample for liquid chromatography−mass spectrometry/mass spectrometry (LC-MS/MS) detection. LC-MS/MS analysis was performed using the EASY-nLC 1200-nanometer UHPLC system, Q Exactive HF-X mass spectrometer, and Nanospray Flex (ESI) ion source. We set the ion spray voltage at 2.3 kV and the temperature of ion transfer tube at 320 °C. In addition, data-dependent acquisition mode was used for MS. The full scan range of the MS was m/z 350−1500, the resolution of the primary MS was set at 60 000 (200 m/z), the maximum capacity of C-trap was 3×10^6, and the maximum injection time of C-trap was 20 ms. The parent ion with TOP 40 ionic strength in the whole scan was selected and fragmented by high-energy collisional cleavage (HCD) method for secondary MS detection. The resolution of secondary MS was set to 15 000 (200 m/z), the maximum capacity of C-trap was 1×10^5, the maximum injection time of C-trap was 45 ms, the collision energy of peptide fragmentation was set to 27%, the threshold intensity was set to 2.2×10^4, the dynamic rejection range was set to 20 s, and finally the MS detection raw data were obtained.

Protein Identification, Quantification, and Data Analysis. The protein database of homo_sapiens_uniprot_2020_1_8.fasta (188 386 sequences) was searched for all of the resulting spectra using the Proteome Discoverer 2.2 software (PD2.2, Thermo). The parameters of PD2.2 software were set as follows: (1) the mass tolerance of precursor ion was 10 ppm; (2) the mass tolerance of fragment ion was 0.02 Da; (3) the immobilization modification was alkylation modification of cysteine; (4) the variable modification was oxidation modification of methionine and acetylation modification of N-terminal, allowing a maximum of two missed cut sites. For improving the quality of the analysis results, PD2.2 software further screened the retrieval results according to the following requirements: (1) only plausible peptide spectrum matches (PSMs) (peptide spectrum with a confidence level of 99% or higher) and proteins (proteins containing at least one unique peptide) were retained and (2) false discovery rate (FDR) validation was done, and peptides and proteins with FDR greater than 1% were discarded.

Statistical analysis of protein quantification results was performed by T-test, and proteins with significant differences in quantification between the groups were defined as differentially expressed proteins ($p < 0.05$, |log$_2$FC| > 1.2 [fold change, FC]). Gene Ontology (GO) and IPR functional annotations (including Pfam, PRINTS, ProDom, SMART,
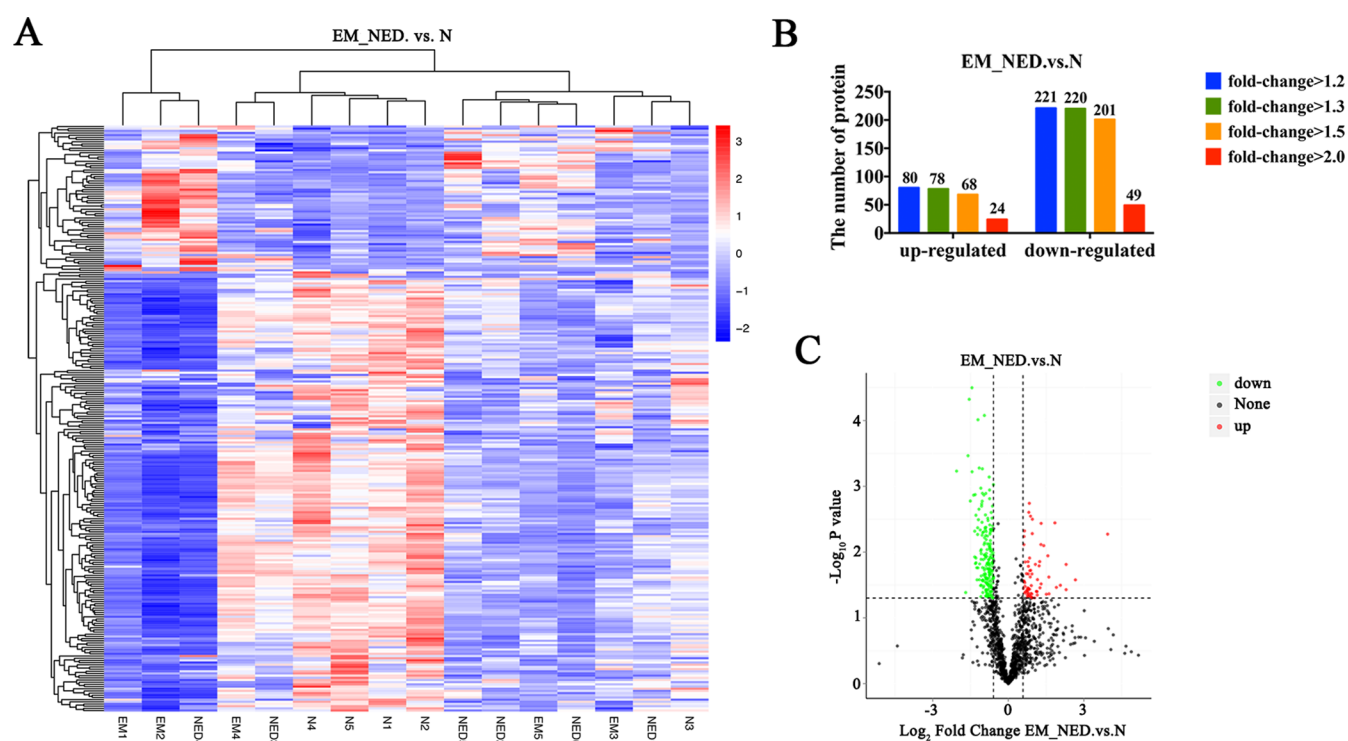
Figure 1. Comparison of encephalitis patients (EM_NED) and normal subjects. (A) Heatmap of the DEPs. (B) Number of up- and downregulated proteins with different fold changes. (C) Volcano plot of log$_2$FC showing a large number of DEPs.

ProSite, PANTHER databases) were performed using InterProScan software. Functional protein family and pathway analysis of the identified proteins was performed using Cluster of Orthologous Groups of proteins (COG) and Kyoto Encyclopedia of Genes and Genomes (KEGG). The volcano plot analysis, clustering heatmap analysis, and pathway enrichment analysis of GO, IPR, and KEGG were performed for differentially expressed proteins (DEPs), and potential protein−protein interactions were predicted using STRING DB software (http://STRING.embl.de/).

Detection of NRXN3, NFASC, NLGN2, and LRRC4B Proteins Using ELISA. First, the CSF samples were centrifuged 200 μL from the −80 °C refrigerator for 20 min at 4 °C (2000g), and the supernatant was removed and labeled. Three subwells were prepared for each sample, with blank wells, standard wells, and samples to be tested, respectively. Then, 50 μL of each diluted standard concentration (16, 8, 4, 2, 1, 0 ng/mL) was added to the six standard wells in turn, one of which was used as a blank control. The remaining sample wells were left empty, and 40 μL of sample diluent was added first, then 10 μL of CSF sample was added to the bottom of the wells of the enzyme plate and mixed with gentle shaking. Then, 100 μL of enzyme standard reagents (NRXN3, NFASC, NLGN2, LRRC4B) was added to each well (except the blank wells), and the membrane was sealed and reacted in a constant-temperature chamber at 37 °C for 60 min. The sealing membrane was removed, the liquid in the wells was shaken dry, and the wells were washed five times with washing solution and patted dry. Each well was added with 100 μL of ABC working solution (50 μL liquid A and 50 μL liquid B) and mixed with gentle shaking for 15 min in a constant-temperature chamber at 37 °C. After that, 50 μL of termination solution was added to each well, and the color changed from blue to yellow. Finally, the wells were zeroed

with blank wells and the optical density (OD) value of each well at 450 nm was measured with an enzyme marker within 15 min of the addition of the termination solution. The average absorbance and concentration of each standard (diluted five times) were plotted using the curve fitting software "Curve Expert 1.3" to create the curve, and the concentration (ng/ mL) of each sample was calculated using this as the standard curve (correlation coefficient should be at least 0.98).

■ RESULTS

Global Proteomic Analysis of EM_NED and N Groups. To identify proteins that were up- or downregulated between encephalitis patients and normal subjects, the label-free quantitative proteomics was performed on the collected CSF samples (Figure 1A). A total of 1377 proteins were identified, including 250 upregulated DEPs and 691 downregulated DEPs (Figure 1B and Table 1). As shown, downregulated proteins were in the majority by comparing the differential proteins of EM_NED and N groups (Figure 1C).

Table 1. Differential Proteins Analysis

compared samples	no. of total quant.	regulated type	fold change			
			>1.2	>1.3	>1.5	>2.0
EM_NED vs N	1377	upregulated	80	78	68	24
		downregulated	221	220	201	49

Common Function Database Annotation. The identified proteins were annotated with common functional databases, including the COG database, GO database, and KEGG database. The top 10 biological processes (BPs) were proteolysis, cell adhesion, oxidation−reduction process, homophilic cell adhesion via plasma membrane adhesion
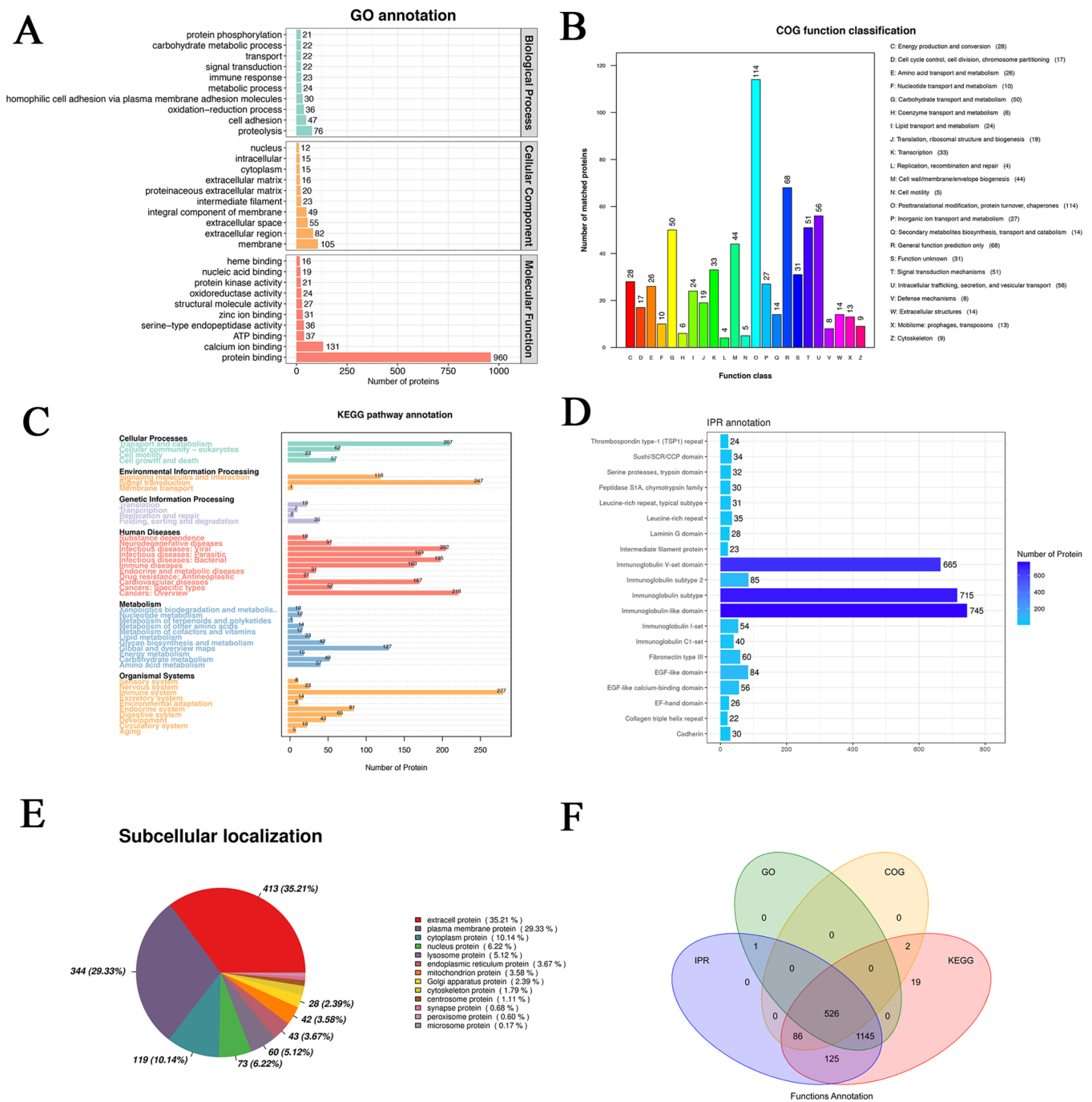
Figure 2. Functional analysis of differential proteins. (A) GO annotation, (B) COG function classification, (C) KEGG pathway annotation, (D) IPR annotation, (E) subcellular localization, and (F) functional annotation with Venn diagrams.

molecules, metabolic process, immune response, signal transduction, transport, carbohydrate metabolic process, and protein phosphorylation (Figure 2A). The top 10 cellular components (CCs) were membrane, extracellular region, extracellular space, integral component of membrane, intermediate filament, proteinaceous extracellular matrix, extracellular matrix, cytoplasm, intracellular, and nucleus (Figure 2A). The top 10 molecular functions (MFs) were protein binding, calcium-ion binding, ATP binding, structural molecule activity, oxidoreductase activity, protein kinase activity, nucleic acid binding, and heme binding (Figure 2A).

Functional classification was obtained according to the function annotation provided by the COG database. The top

10 COG functions were [O] posttranslational modification, protein turnover, chaperones (114 proteins), [R] general function prediction only (68 proteins), [U] intracellular trafficking, secretion, and vesicular transport (56 proteins), [T] signal transduction mechanisms (51 proteins), [G] carbohydrate transport and metabolism (50 proteins), [M] cell wall/membrane/envelope biogenesis (44 proteins), [K] transcription (33 proteins), [S] function unknown (31 proteins), [C] energy production and conversion (28 proteins), and [P] inorganic ion transport and metabolism (27 proteins) (Figure 2B).

The results of the annotation of differentially expressed genes were categorized according to the type of pathway in
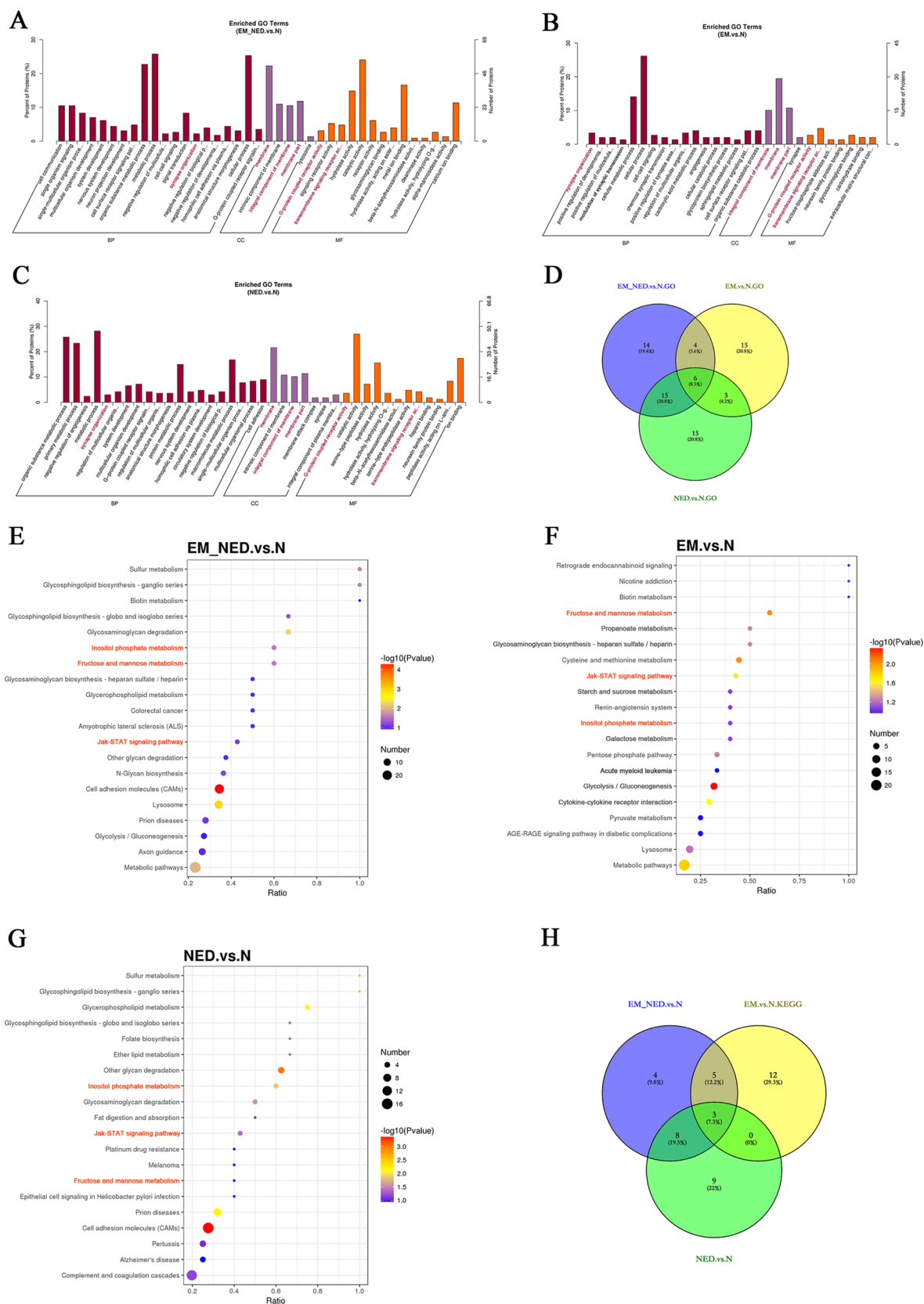
Figure 3. GO and KEGG analysis. (A) Enriched GO terms between the EM_NED and N groups. (B) Enriched GO terms between the EM and N groups. (C) Enriched GO terms between the NED and N groups. (D) Overlap of the enriched GO function among the EM, EM_NED, and N groups. (Six of these intersection functions were highlighted in red in (A−C).) (E) KEGG terms between the EM_NED and N groups. (F) KEGG terms between the EM and N groups. (G) KEGG terms between the NED and N groups. (H) Overlap of the KEGG function among the EM, EM_NED, and N groups. (Three of these intersection functions were highlighted in orange in (E−G).)
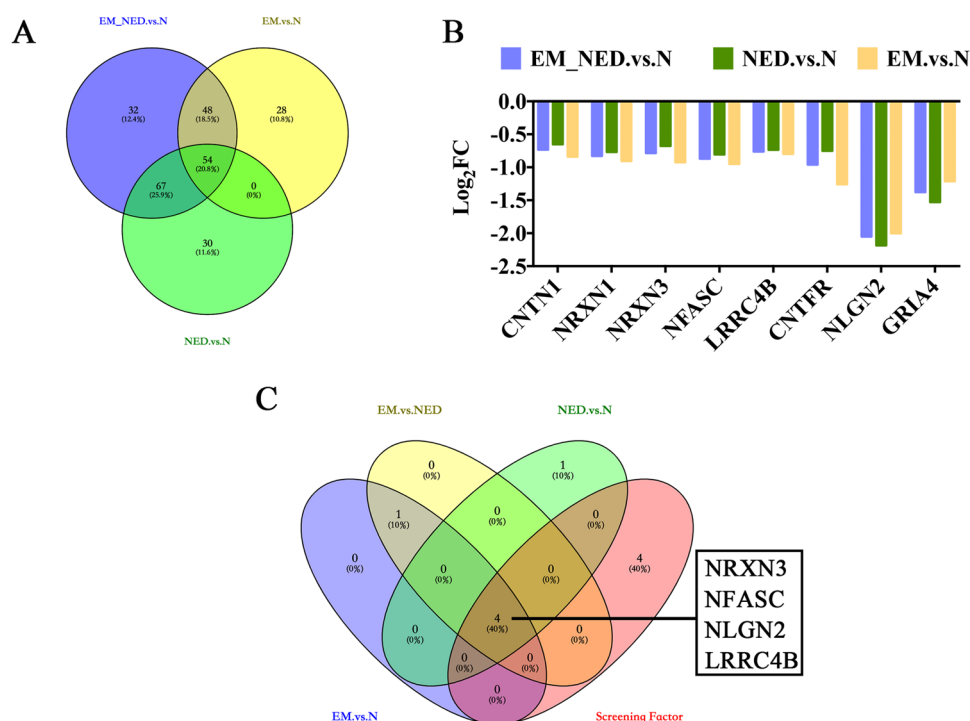
Figure 4. Protein screening. (A) Venn's plots of downregulated proteins. (B) Log$_2$FC of neural-related 8 of the 54 downregulated proteins in the overlap of the EM_NED vs N, NED vs N, and EM vs N. (C) Venn's plots of upregulated proteins among EM vs N, NED vs N, and EM vs NED associated with synapse organization and neural-related 8 proteins.

KEGG. The cellular processes were transport and catabolism (207), cellular community eukaryotes (62), cell growth and death (57), and cell motility (23) (Figure 2C). The environmental information processing included signal transduction (247), signaling molecules and interaction (116), and membrane transport (1) (Figure 2C). The genetic information processing included folding, sorting, and degradation (35), translation (19), transcription (7), and replication and repair (2) (Figure 2C). Human diseases included cancers: overview (216), infectious disease: viral (202), infectious diseases: bacterial (195), infectious diseases: parasitic (169), cardiovascular diseases (167), immune diseases (160), cancers: specific types (52), neurodegenerative diseases (51), endocrine and metabolic diseases (31), drug resistance: antineoplastic (21), and substance dependence (19) (Figure 2C). Global and overview maps (127), carbohydrate metabolism (49), glycan biosynthesis and metabolism (42), amino acid metabolism (37), lipid metabolism (23), energy metabolism (15), metabolism of other amino acids (14), metabolism of cofactors and vitamins (12), nucleotide metabolism (12), xenobiotics biodegradation and metabolism (10), and metabolism of terpenoids and polyketides (1) were included in the metabolism (Figure 2C). The organismal systems included immune system (227), endocrine system (81), digestive system (65), development (43), nervous system (23), circulatory system (19), excretory system (14), sensory system (8), environmental adaptation (8), and aging (5) (Figure 2C).

The top 10 IPR were immunoglobulin-like domain (745 proteins), immunoglobulin subtype (715 proteins), immunoglobulin V-set domain (665 proteins), immunoglobulin subtype 2 (85 proteins), EGF-like domain (84 proteins), fibronectin type III (60 proteins), EGF-like calcium-binding domain (56 proteins), immunoglobulin I-set (54 proteins),

immunoglobulin C1-set (40 proteins), and leucine-rich repeat (35 proteins) (Figure 2D).

In addition, the top 10 subcellular localization of DEPs were extra cell protein (35.21%), plasma membrane protein (29.33%), cytoplasm protein (10.4%), nucleus protein (6.22%), lysosome protein (5.12%), endoplasmic reticulum protein (3.67%), mitochondrion protein (3.58%), Golgi apparatus protein (2.39%), cytoskeleton protein (1.79%), and centrosome protein (1.11%) (Figure 2E).

The Venn diagram demonstrated that there were 526 differentially expressed proteins in the overlap of the previous results (Figure 2F).

GO and KEGG Analysis. As shown, the enriched GO and KEGG terms of EM_NED vs N, EM vs N, and NED vs N were presented, and the six GO intersection functions were highlighted in red (Figure 3A−D) and the three intersection signaling pathways were highlighted in orange (Figure 3E−H). The results indicated that the enriched GO term of EM_NED vs N was synapse organization in BP; membrane, integral component of membrane, and membrane part in CC; and G-protein-coupled receptor signaling pathway and transmembrane signaling receptor activity in MF. In addition, the enriched KEGG terms of EM_NED vs N were fructose and mannose metabolism, inositol phosphate metabolism, and Jak-STAT signaling pathway.

NLGN2 and LRRC4B Proteins Were Upregulated in NED. Results showed that there were 54 upregulated proteins in the overlap of the EM_NED vs N, EM vs N, and NED vs N (Figure 4A). Furthermore, we identified eight neurological function-related proteins associated with the development of encephalitis, including CNTN1, NRXN1, NRXN3, NFASC, LRRC4B, CNTFR, NLGN2, and GRIA4 (Figure 4B). In addition, we further screened synaptic-related proteins in neural function, including NRXN3, NFASC, NLGN2, and

LRRC4B (Figure 4C). Besides, the expression of four proteins was further verified by ELISA. It was suggested that the expression of NLGN2 and LRRC4B proteins was significantly upregulated in NED compared to normal groups (Figure 5C,D; p = 0.016, 0.025), while the expression of NRXN3 and NFASC proteins in CSF of the three groups was not significantly different (Figure 5A,B; p > 0.05).
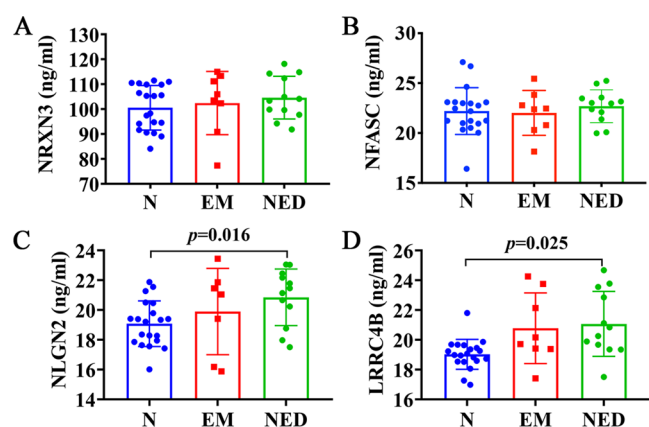

Figure 5. ELISA validation of NRXN3, NFASC, NLGN2, and LRRC4B proteins in N, EM, and NED groups. (A−D) Comparison of NRXN3, NFASC, NLGN2, and LRRC4B proteins in the three groups.

■ DISCUSSION

CSF is connected to the somatic circulation via the intracerebral venous system, and more information about the pathology of encephalitis can be obtained by studying the DEPs in CSF of encephalitis patients and healthy individuals, and these DEPs are useful as candidate markers for encephalitis diagnosis for further studies. In this research, the proteomic study was performed on a total of 11 CSF samples, and 1377 proteins were found to be significantly differentially expressed in the overlap of encephalitis patients and healthy individuals.

Encephalitis was linked to the human Zika virus in a previous study, the researchers identified the dysregulated astrocyte proteins that span diverse functions and signaling pathways including synaptic control.[13] Besides, a review on the proteomic analysis of CSF from rabies infection also illustrated that it is related to synaptic and neurotransmission.[14] Inhibiting neuroinflammation is an important strategy in the treatment of brain disease. Xia et al. demonstrated the important role of the dopamine receptor as an important G-protein-coupled receptor in inflammation-associated glial cells.[15] Chen et al. found that the interaction of high-mobility group box 1 protein and transmembrane receptor would lead to a cascade amplification of inflammatory responses.[16] Furthermore, our study also revealed that synapse organization, membrane, integral component of membrane, membrane part, G-protein-coupled receptor signaling pathway, and transmembrane signaling receptor activity were the enriched functions of encephalitis patients and healthy individuals in GO functional annotation. In the study, the KEGG annotation suggested that fructose and mannose metabolism, inositol phosphate metabolism, and Jak-STAT signaling pathway were the enriched signaling pathways among the EM, NED, and N groups. Notably, fructose and mannose metabolism and inositol monophosphatase have been identified in the CSF,[17,18] but no studies reported that it is associated with encephalitis. Additionally, the findings on Jak-STAT signaling pathway associated with the encephalitis were also supported by previous reports.[19−21]

Through label-free quantitative proteomics combined with GO and KEGG analysis, we identified four downregulated encephalitis-related neurological synapse proteins, including NRXN3, NFASC, LRRC4B, and NLGN2. Notably, the NLGN2 and LRRC4B proteins were most dramatically expressed in the CSF. Neurexins (NRXN) are a class of synaptic adhesion molecules that are essential in the formation and establishment of synaptic structures and the maintenance of synaptic function.[22] It has been found that abnormalities in presynaptic NRXN3 expression may increase inflammation in AD brain neurons, and autoantibodies to NRXN3 (neurexin-3) cause alterations in synaptic development in a novel autoimmune encephalitis.[23,24] Additionally, NFASC (neurofascin) is a transmembrane protein that is critical in the development of the nervous system and in the functional nodes of Ranvier.[25] LRRC4B (Leucine Rich Repeat Containing 4B), a synaptic adhesion protein, can regulate the formation of excitatory synapses,[26] which have not been reported in encephalitis. In this study, we found that LRRC4B was significantly upregulated in the CSF of encephalitis patients. Besides, Neuroligin (NLGN) is a postsynaptic cell adhesion protein molecule that interacts with NRXN to participate in synapse formation and function.[27] NLGN2 can be found in the central nervous system and is closely associated mainly with inhibitory GABA aminobutyric acid signaling, which is essential for maintaining excitation−inhibition balance in the brain.[28] Chugh et al.[29] observed inhibitory adhesion molecules NLGN2 (neuroligin-2) and NFASC and potassium chloride co-transporter KCC2 in the brain inflammation studies of mice. Katzman et al.'s study[30] revealed the functions of the excitatory and inhibitory synaptic proteins neuroligin 1 (NLGN1) and NLGN2 in PFC in the regulation of memory formation and memory intensity, helping to suggest new protocols for the treatment of excitatory/inhibitory imbalances associated with neuropsychiatric disorders. In addition, in animal models, the abnormal expression of NLGN2 resulted in changes in anxiety, developmental delay, motor dysregulation, social impairment, and social competence.[31] The analysis of NLGN transcriptional genes in patients who died from major depressive disorder suggested a downregulation of NLGN2 expression.[32] Moreover, the results of proteomic assays showed downregulation of the expression of axon-related proteins (NRXN3, NLGN2, NFASC, LRRC4B). This might be due to the direct damage of axonal tissue by inflammation, which disrupted the expression of axon-related proteins and led to the imbalance of excitation and inhibition, resulting in clinical manifestations such as motor impairment and mental behavior abnormalities. This was consistent with the good therapeutic effect of neurotrophic drugs in most patients. Furthermore, based on label-free proteomics, ELISA was further applied to validate the NRXN3, NLGN2, NFASC, and LRRC4B proteins. It suggested that the expression of NLGN2 and LRRC4B proteins was significantly higher in the NED group than in the N group. This indicated that NLGN2 and LRRC4B were involved in the pathogenesis of encephalitis. In contrast, the results of our proteomics study showed significantly downregulated NLGN2 and LRRC4B in patients with encephalitis, while ELISA showed an upregulation, and the exact

mechanism leading to its increased level is not clear. It has been confirmed that NLGN2 is part of the constituent inhibitory synapses and is associated with GABA aminobutyric acid signaling, and its upregulation in expression leads to increased inhibitory effects at synapses.[33] It is thought that the imbalance of excitatory and inhibitory signals such as GABA aminobutyric acid mediated by early damage axons in infection may be relevant, and further studies of related signaling pathways are needed.

However, considering the possible limitations of this study in terms of design, technique, and analytical strategy, further validation using multiomics and multiple validation methods were needed to confirm the reliability of these findings. In summary, these findings demonstrated that NLGN2 and LRRC4B proteins were upregulated in the NED group, which could be further investigated as candidate markers for encephalitis diagnosis.

AUTHOR INFORMATION

Corresponding Authors

Ting-Hua Wang − *Institute of Neurological Disease, West China Hospital, Sichuan University, Chengdu 610041, Sichuan, China;* orcid.org/0000-0003-2012-8936; Email: Wangth_email@163.com

Chang-Yin Yu − *Department of Neurology, Affiliated Hospital of Zunyi Medical University, Guizhou 550000, China;* Email: 775886450@qq.com

Authors

Liu-Lin Xiong − *Department of Anesthesiology, Affiliated Hospital of Zunyi Medical University, Guizhou 550000, China*

Lu-Lu Xue − *Institute of Neuroscience, Kunming Medical University, Kunming 650031, China*

Yan-Jun Chen − *Institute of Neurological Disease, West China Hospital, Sichuan University, Chengdu 610041, Sichuan, China*

Ruo-Lan Du − *Institute of Neurological Disease, West China Hospital, Sichuan University, Chengdu 610041, Sichuan, China*

Qian Wang − *Department of Neurology, Affiliated Hospital of Zunyi Medical University, Guizhou 550000, China*

Song Wen − *Department of Anesthesiology, Affiliated Hospital of Zunyi Medical University, Guizhou 550000, China*

Lin Zhou − *Department of Anesthesiology, Affiliated Hospital of Zunyi Medical University, Guizhou 550000, China*

Tao Liu − *Department of Neurology, Affiliated Hospital of Zunyi Medical University, Guizhou 550000, China*

Complete contact information is available at:
https://pubs.acs.org/10.1021/acsomega.1c00367

Author Contributions

[⊥]L.-L. Xiong and L.-L. Xue contributed equally to this work.

Notes

The authors declare no competing financial interest.

REFERENCES

(1) Collao-Parra, J. P.; Romero-Urra, C.; Delgado-Derio, C. Autoimmune encephalitis. A review. *Rev. Med. Chile* **2018**, *146*, 351−361.

(2) Frackowiak, M.; Easton, A.; Michael, B. D. Encephalitis. *Br. J. Hosp. Med.* **2019**, *80*, No. C50.

(3) Ellul, M.; Solomon, T. Acute encephalitis - diagnosis and management. *Clin. Med.* **2018**, *18*, 155−159.

(4) Filis, A. K.; Aghayev, K.; Vrionis, F. D. Cerebrospinal Fluid and Hydrocephalus: Physiology, Diagnosis, and Treatment. *Cancer Control* **2017**, *24*, 6−8.

(5) Sathe, G.; Na, C. H.; Renuse, S.; Madugundu, A.; Albert, M.; Moghekar, A.; Pandey, A. Phosphotyrosine profiling of human cerebrospinal fluid. *Clin. Proteomics* **2018**, *15*, No. 29.

(6) Heywood, W. E.; Galimberti, D.; Bliss, E.; Sirka, E.; Paterson, R. W.; Magdalinou, N. K.; Carecchio, M.; Reid, E.; Heslegrave, A.; Fenoglio, C.; Scarpini, E.; Schott, J. M.; Fox, N. C.; Hardy, J.; Bhatia, K.; Heales, S.; Sebire, N. J.; Zetterberg, H.; Mills, K. Identification of novel CSF biomarkers for neurodegeneration and their validation by a high-throughput multiplexed targeted proteomic assay. *Mol. Neurodegener.* **2015**, *10*, No. 64.

(7) Macron, C.; Lane, L.; Núñez Galindo, A.; Dayon, L. Deep Dive on the Proteome of Human Cerebrospinal Fluid: A Valuable Data Resource for Biomarker Discovery and Missing Protein Identification. *J. Proteome Res.* **2018**, *17*, 4113−4126.

(8) Taibi, L.; Boursier, C.; Clodic, G.; Bolbach, G.; Bénéteau-Burnat, B.; Vaubourdolle, M.; Baudin, B. Search for biomarkers of neurosarcoidosis by proteomic analysis of cerebrospinal fluid. *Ann. Biol. Clin.* **2017**, *75*, 393−402.

(9) Pan, S.; Wang, Y.; Quinn, J. F.; Peskind, E. R.; Waichunas, D.; Wimberger, J. T.; Jin, J.; Li, J. G.; Zhu, D.; Pan, C.; Zhang, J. Identification of glycoproteins in human cerebrospinal fluid with a complementary proteomic approach. *J. Proteome Res.* **2006**, *5*, 2769−2779.

(10) Sickmann, A.; Dormeyer, W.; Wortelkamp, S.; Woitalla, D.; Kuhn, W.; Meyer, H. E. Identification of proteins from human cerebrospinal fluid, separated by two-dimensional polyacrylamide gel electrophoresis. *Electrophoresis* **2000**, *21*, 2721−2728.

(11) Altelaar, A. F.; Munoz, J.; Heck, A. J. Next-generation proteomics: towards an integrative view of proteome dynamics. *Nat. Rev. Genet.* **2013**, *14*, 35−48.

(12) Aslam, B.; Basit, M.; Nisar, M. A.; Khurshid, M.; Rasool, M. H. Proteomics: Technologies and Their Applications. *J. Chromatogr. Sci.* **2017**, *55*, 182−196.

(13) Sher, A. A.; Glover, K. K. M.; Coombs, K. M. Zika Virus Infection Disrupts Astrocytic Proteins Involved in Synapse Control and Axon Guidance. *Front. Microbiol.* **2019**, *10*, No. 596.

(14) Mehta, S. M.; Banerjee, S. M.; Chowdhary, A. S. Postgenomics biomarkers for rabies—the next decade of proteomics. *OMICS* **2015**, *19*, 67−79.

(15) Xia, Q. P.; Cheng, Z. Y.; He, L. The modulatory role of dopamine receptors in brain neuroinflammation. *Int. Immunopharmacol.* **2019**, *76*, No. 105908.

(16) Chen, X.; Wu, S.; Chen, C.; Xie, B.; Fang, Z.; Hu, W.; Chen, J.; Fu, H.; He, H. Omega-3 polyunsaturated fatty acid supplementation attenuates microglial-induced inflammation by inhibiting the HMGB1/TLR4/NF-κB pathway following experimental traumatic brain injury. *J. Neuroinflammation* **2017**, *14*, No. 143.

(17) Rastedt, W.; Blumrich, E. M.; Dringen, R. Metabolism of Mannose in Cultured Primary Rat Neurons. *Neurochem. Res.* **2017**, *42*, 2282−2293.

(18) Atack, J. R.; Rapoport, S. I.; Varley, C. L. Characterization of inositol monophosphatase in human cerebrospinal fluid. *Brain Res.* **1993**, *613*, 305−308.

(19) Wu, Y.; Xu, J.; Xu, J.; Zheng, W.; Chen, Q.; Jiao, D. Study on the mechanism of JAK2/STAT3 signaling pathway-mediated inflammatory reaction after cerebral ischemia. *Mol. Med. Rep.* **2018**, *17*, 5007−5012.

(20) Lin, R. J.; Chang, B. L.; Yu, H. P.; Liao, C. L.; Lin, Y. L. Blocking of interferon-induced Jak-Stat signaling by Japanese encephalitis virus NS5 through a protein tyrosine phosphatase-mediated mechanism. *J. Virol.* **2006**, *80*, 5908−5918.

(21) Sasaki, T.; Kuwata, R.; Hoshino, K.; Isawa, H.; Sawabe, K.; Kobayashi, M. Argonaute 2 Suppresses Japanese Encephalitis Virus Infection in *Aedes aegypti*. *Jpn. J. Infect. Dis.* **2017**, *70*, 38−44.

(22) Hu, Z.; Xiao, X.; Zhang, Z.; Li, M. Genetic insights and neurobiological implications from NRXN1 in neuropsychiatric disorders. *Mol. Psychiatry* **2019**, *24*, 1400−1414.

(23) Gresa-Arribas, N.; Planagumà, J.; Petit-Pedrol, M.; Kawachi, I.; Katada, S.; Glaser, C. A.; Simabukuro, M. M.; Armangué, T.; Martínez-Hernández, E.; Graus, F.; Dalmau, J. Human neurexin-3α antibodies associate with encephalitis and alter synapse development. *Neurology* **2016**, *86*, 2235−2242.

(24) Hishimoto, A.; Pletnikova, O.; Lang, D. L.; Troncoso, J. C.; Egan, J. M.; Liu, Q. R. Neurexin 3 transmembrane and soluble isoform expression and splicing haplotype are associated with neuron inflammasome and Alzheimer's disease. *Alzheimers Res. Ther.* **2019**, *11*, No. 28.

(25) Monfrini, E.; Straniero, L.; Bonato, S.; Monzio Compagnoni, G.; Bordoni, A.; Dilena, R.; Rinchetti, P.; Silipigni, R.; Ronchi, D.; Corti, S.; Comi, G. P.; Bresolin, N.; Duga, S.; Di Fonzo, A. Neurofascin (NFASC) gene mutation causes autosomal recessive ataxia with demyelinating neuropathy. *Parkinsonism Relat. Disord.* **2019**, *63*, 66−72.

(26) Linhoff, M. W.; Laurén, J.; Cassidy, R. M.; Dobie, F. A.; Takahashi, H.; Nygaard, H. B.; Airaksinen, M. S.; Strittmatter, S. M.; Craig, A. M. An unbiased expression screen for synaptogenic proteins identifies the LRRTM protein family as synaptic organizers. *Neuron* **2009**, *61*, 734−749.

(27) Kasem, E.; Kurihara, T.; Tabuchi, K. Neurexins and neuropsychiatric disorders. *Neurosci. Res.* **2018**, *127*, 53−60.

(28) Bang, M. L.; Owczarek, S. A matter of balance: role of neurexin and neuroligin at the synapse. *Neurochem. Res.* **2013**, *38*, 1174−1189.

(29) Chugh, D.; Ali, I.; Bakochi, A.; Bahonjic, E.; Etholm, L.; Ekdahl, C. T. Alterations in Brain Inflammation, Synaptic Proteins, and Adult Hippocampal Neurogenesis during Epileptogenesis in Mice Lacking Synapsin2. *PLoS One* **2015**, *10*, No. e0132366.

(30) Katzman, A.; Alberini, C. M. NLGN1 and NLGN2 in the prefrontal cortex: their role in memory consolidation and strengthening. *Curr. Opin. Neurobiol.* **2018**, *48*, 122−130.

(31) Parente, D. J.; Garriga, C.; Baskin, B.; Douglas, G.; Cho, M. T.; Araujo, G. C.; Shinawi, M. Neuroligin 2 nonsense variant associated with anxiety, autism, intellectual disability, hyperphagia, and obesity. *Am. J. Med. Genet.* **2017**, *173*, 213−216.

(32) Heshmati, M.; Aleyasin, H.; Menard, C.; Christoffel, D. J.; Flanigan, M. E.; Pfau, M. L.; Hodes, G. E.; Lepack, A. E.; Bicks, L. K.; Takahashi, A.; Chandra, R.; Turecki, G.; Lobo, M. K.; Maze, I.; Golden, S. A.; Russo, S. J. Cell-type-specific role for nucleus accumbens neuroligin-2 in depression and stress susceptibility. *Proc. Natl. Acad. Sci. U.S.A.* **2018**, *115*, 1111−1116.

(33) Rothwell, P. E.; Fuccillo, M. V.; Maxeiner, S.; Hayton, S. J.; Gokce, O.; Lim, B. K.; Fowler, S. C.; Malenka, R. C.; Südhof, T. C. Autism-associated neuroligin-3 mutations commonly impair striatal circuits to boost repetitive behaviors. *Cell* **2014**, *158*, 198−212.